CFD Modelling of Potroom Ventilation

Vanderlei Gusberti[1], Dagoberto Schubert Severo[2], Elkjaer Ferreira Braz[3] and Marc Dupuis[4]
1. PhD Engineer
2. Director
CAETE Engenharia, Porto Alegre, Brazil
3. Engineer
CBA Companhia Brasileira de Aluminio, Aluminio, Brazil
4. Consultant
GeniSim, Jonquière, Canada
Corresponding author: dagoberto@caetebr.com
https://doi.org/10.71659/icsoba2024-al052

Abstract

In the industrial aluminium smelting process, hundreds of cells are placed inside the potroom building. Ventilation of this space is primarily provided by natural convection, where the electrolysis cells are the heat sources. Occasionally, the ventilation is also affected by winds accessing the building through its openings and windows.

In previous studies, the simulation of potroom ventilation has been shown to be a difficult task, particularly regarding the appropriate choice of the turbulence model, which greatly affected the predicted flow pattern. Difficulties in finding a turbulence model that can correctly represent the thermal plume that forms above the cells and rises towards the roof have been reported. Two-equation turbulence models such as k-epsilon and k-omega have been shown to be inadequate. The Reynolds flux model was found to give good results, but this turbulence model is no longer supported by the major commercial codes, allegedly due to its limited range of flows applicability.

In this work, the physical model studied by Dupuis [1] is revisited. The buoyant flow numerical simulations of the physical model are compared with the experimental results. Both Large Eddy Simulation (LES) and Detached Eddy Simulation (DES) are intrinsically transient turbulence models, and both model results are shown to be representative when compared with the experimental work. Finally, DES is used in an industrial potroom ventilation simulation. DES proved to be the most suitable choice of turbulence modelling for industrial potrooms while maintaining accuracy of the results, because it requires less time and space discretization than LES.

Keywords: Potroom ventilation, Buoyant flow, Turbulence modelling, Detached Eddy Simulation, Large Eddy Simulation.

1. Introduction to Potroom Ventilation

Industrial aluminium electrolysis is an intensive energy-consuming process, producing a huge amount of heat dissipation by the cells as well as gaseous contaminants originated from electrolysis or the parallel reactions associated with raw materials impurities (such as SO_2 and HF). In modern smelters, the adequate ventilation of the potroom building is crucial in many aspects:

- At the working level, fresh air at ambient temperature must be supplied for the thermal comfort of workers. In addition, the gases produced in the cell cavity must be removed from the working area, bringing the contamination levels of breathing air within a standard acceptable range.

- The cell heat removal has to be efficient in order to maintain the shell, busbars, cell hoods, and all adjacent equipment in adequate temperatures; otherwise, the cell parts can overheat, potentially leading to catastrophic failure.
- Environmental regulations are becoming tighter in many regions of the world for the benefit of workers, the external environment, and society. This is demanding better solutions for pot gas collection, gas treatment, and heat dissipation.

As a general concept, the potroom contains one or two rows of cells. Intensive heat generation is produced by each cell (typically in the order of 500–1000 kW). This thermal power is then lost by means of natural convection and an air "plume" is formed towards the building roof. Usually, the potroom presents a "roof vent" geometry specially designed to extract heat and gases as efficiently as possible while preventing rain and snow to enter. Potroom windows and openings strongly influence the resulting flow intensity, and these openings have to be designed accordingly. Another important factor is the wind regime to which the potroom is subjected during the year. Wind can help or hinder natural convection efficiency depending on its intensity and direction.

2. Literature Review: Turbulence Models Applied to Potroom Ventilation

The flow generated by natural convection in the potroom is intensely turbulent. Turbulence is an intrinsic transient phenomenon present in fluid flow, characterised by chaotic fluctuations in flow velocities and other transported quantities (pressure, temperature, concentration) both in time and space. Turbulent flows present intermittent formation and collapse of eddies of various sizes over time. Numerical simulation of turbulent flows is challenging and has been extensively studied by academic and industrial analysts. Many turbulence models have been developed over the years, each with its own assumptions and applicability limitations. Moreover, there is no universal turbulence model, and each Computational Fluid Dynamics (CFD) study has to carefully choose a suitable one depending on the simulations' objectives and expected flow characteristics.

Turbulence models can be divided into the following categories:

- Reynolds Averaged Navier-Stokes (RANS). Steady state models, aiming to statistically describe the turbulence as an average over time. Turbulence acts as an increase in the flow viscosity (turbulent viscosity field is created). Example of one-equation formulation: Spallart-Allmaras. Examples of two-equations formulations: k-epsilon, k-omega, Shear Stress Transport (SST). Example of six-equations formulations: Reynolds Stresses Model (RSM).
- Unsteady Reynolds Averaged Navier-Stokes (URANS). The same formulation used in RANS, but including the transient term. Some fluctuations in the flow can be described depending on the mesh and timestep resolution.
- Large Eddy Simulation (LES). Eddies larger than the mesh are directly simulated, and eddies smaller than the mesh are modelled with the "sub grid scale model" (SGS modelling). This turbulence modelling approach is always transient, and the computational cost is high because it requires fine spatial and temporal discretization.
- Detached Eddy Simulation (DES). This is a hybrid model where larger eddies are calculated as LES and the rest of the flow is modelled using URANS turbulence model, mainly near the wall regions. It is a compromise solution between accuracy and computational cost for industrial applications.

During the last decades of the twentieth century, CFD started to be used as a tool for analysing the potroom ventilation flow [1–3]. At that time, only RANS turbulence models were considered of practical use, in two-dimensional steady state models. In the work presented by Dupuis et al. [1] in 1989, physical model measurements (reproduced in Figure 1) were compared with CFD

predictions. Some two-equations RANS turbulence models were assessed. All modelling results were considered unsatisfactory. The plume shape and the temperature distribution resulted to be different from the physical model measurements. Only in 1993, an adequate representation of the measured flow was achieved [3], at that occasion using the Reynolds Flux Model or Differential Flux Model (RFM or DFM, respectively). In 2001 [4], the same model was expanded for RANS 3D. DFM is a 10 equations RANS turbulence model that is not supported anymore by the mainstream commercial codes such as FLUENT or CFX. Those software providers alleged that the DFM turbulence model was not suitable for a wide range of flows, and a better approach would be to use LES or DES simulations, which are computationally costly, but may be feasible with nowadays' resources.

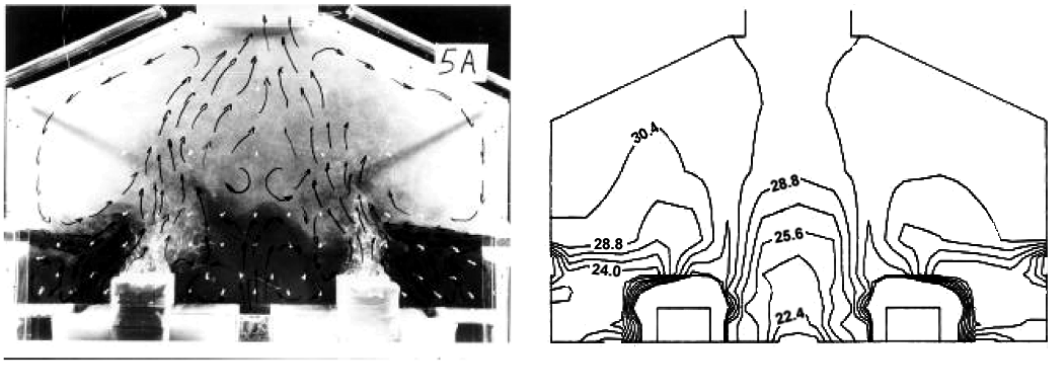

Smoke concentration **Isotherms**

Figure 1. Experimental data, reproduced from Dupuis et al. [3].

Despite the limitations of the two-equations RANS models demonstrated in earlier articles, some modelling works continued to use these approaches, such as the k-omega and the k-epsilon models [5–7]. in the modelling and experimental work described by Menet et al. [6], the k-epsilon turbulence model was used, and, the authors were apparently satisfied with the results for the objectives of their work. No study or comparisons with other turbulence models have been presented. They also presented only steady state averaged results. In the simulations of potroom ventilation shown by Vershenya et al. [8], the flow solution is steady state but the turbulence modelling approach was not described by the authors.

3. Numerical Simulation of the Physical Model

In this work, the intrinsically transient turbulence models LES and DES are employed for the numerical simulation of the laboratory physical model studied by Dupuis et al. [1, 3]. The aim is to reproduce the experimental data recorded at that time, but using modern CFD turbulence models since the differential flux model has become unavailable in most commercial codes.

3.1 Boundary Conditions Applied

The physical model geometry employed for the experimental data acquisition is shown in Figure 2. It represents a slice of a potroom with two potrows in the same building. Two cells are represented by heat dissipating rectangular blocks. The same boundary conditions used in past articles [1, 3] were applied. The studied case presents five inlets and one outlet.

- Fresh air temperature: 20 °C
- Lateral wall inlet prescribed velocities: 0.284 m/s
- Lateral bottom inlet prescribed velocities: 0.216 m/s
- Central bottom inlet velocity: 0.189 m/s
- Top outlet: fixed static pressure (zero pressure is set)
- Heat generation for each cell block: 75 W

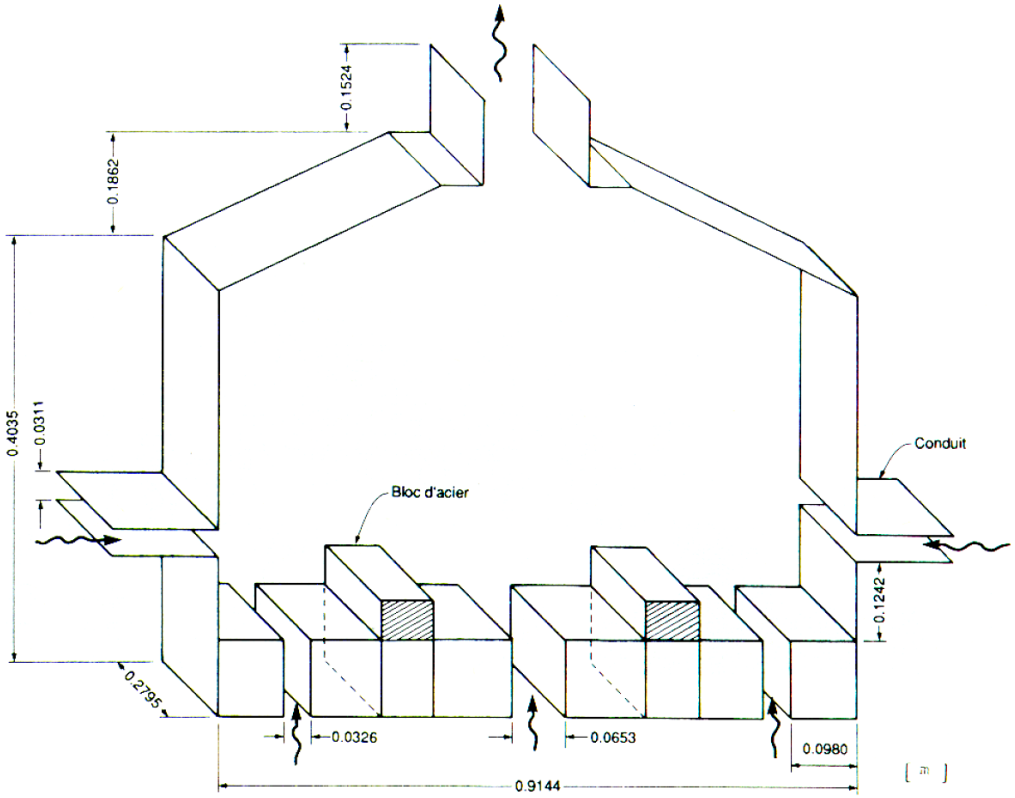

Figure 2. Physical model dimensions, [m], reproduced from Dupuis et al. [1].

Notice that the physical model inlets present prescribed velocities, making the studied flow a mix of natural convection and forced convection flow.

3.2 Turbulence Models Study and Comparisons with Experimental Results

Numerical models were calculated using four different turbulence treatments:

- Case A: Steady state (RANS) SST k-omega, 2D geometry;
- Case B: Transient (URANS) SST k-omega, 3D geometry;
- Case C: Large Eddy Simulation (LES) with Wall-Adapting Local Eddy-Viscosity (WALE) wall treatment, 3D geometry;
- Case D: Hybrid model Detached Eddy Simulation (DES) with SST k-omega, 3D geometry.

Figure 3 presents the air flow results for each case. The vectors represent the time-averaged air velocity obtained in 40 seconds of transient simulation (with exception of Case 1, which is steady state), and the brown surfaces are the formed thermal plume (instantaneous at t = 40 s) where isothermal surfaces at 36 °C are represented.

In cases A and B, the results reproduced the findings described in the literature [1–4]. The widely used two-equation RANS/URANS models produced a strong central stream of hot air towards the roof, and the angle of the plume approaches 45 °. This is in contrast with the experimental data that showed two relatively separated plumes, more verticalized presenting a 15–20 ° inclination with respect to the vertical axis, as shown in Figure 4. The RANS model (Case A) does not converge to a steady state solution in 3D when using the same mesh of Case B, C and D (the same mesh was used in these cases with sufficient refinement in mesh size to allow for the employment of LES and DES turbulence models). Steady state solution was only obtained when

using a coarser 2D mesh. This occurs because the flow is intrinsically transient with large scale eddies. Other RANS models were tested (k-epsilon, standard k-omega, six equations Reynolds Stress) with similar results, which are not reproduced here to avoid repetition.

Cases C and D (LES and DES) present flow pattern results much closer to that of the experimental work, as well as thermal plumes that are visually very similar to the experimental one, presenting an angle with the vertical axis of around 15–20°, as can be seen in the comparison of Figure 5. The DES model was chosen for further comparisons instead of the pure LES because:

- The DES results are considered to be in excellent agreement with the experimental work.
- It requires lower computational effort (around four times faster than LES in this case) as DES is less restrictive in discretization and timestep size. This is important in order to apply the numerical model to geometrically more complex industrial cases.

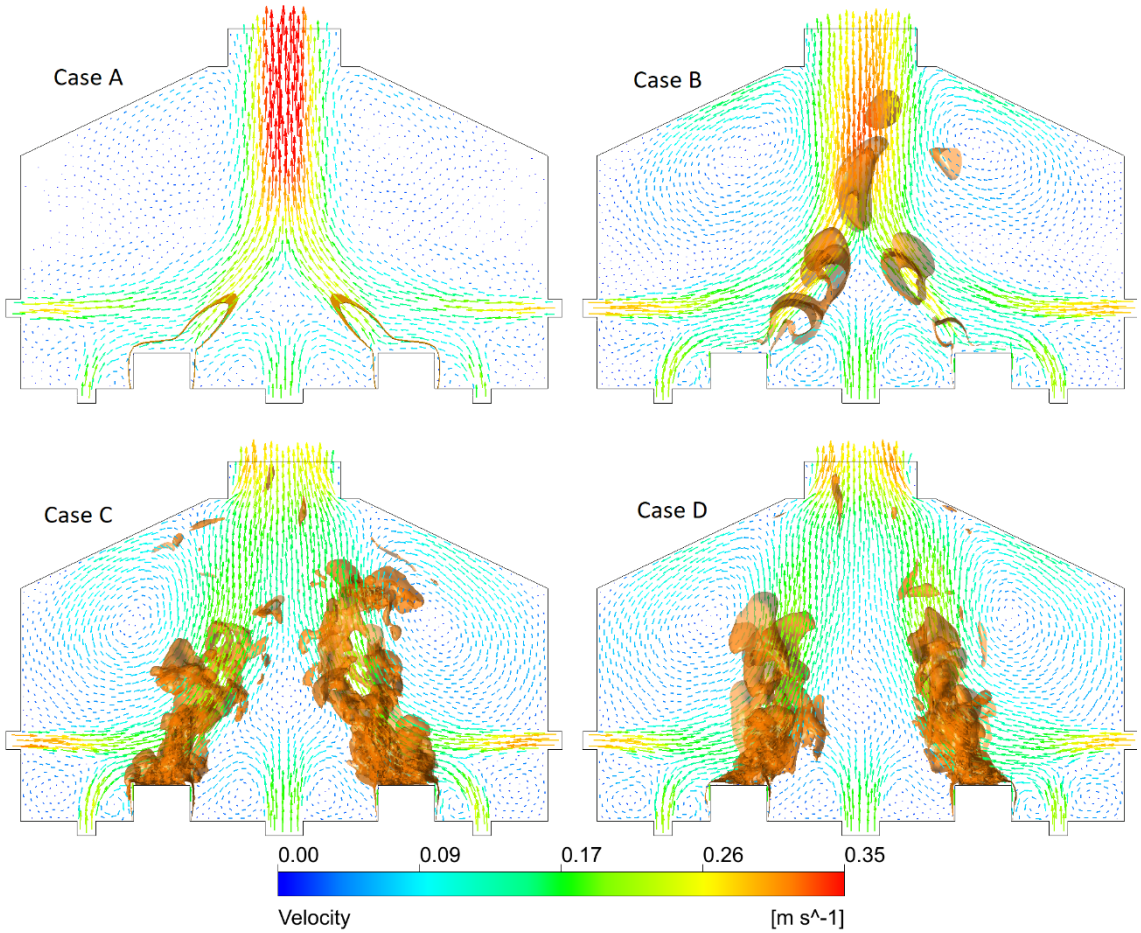

Figure 3. Numerical results comparison. Vectors: time averaged air velocities. Plume: instantaneous isothermal surface at 36 °C.

Figure 6 shows the comparison between the measured and calculated RANS air temperature fields, while the Figure 7 shows a similar comparison between the measured and time-averaged calculated temperature fields using the DES turbulence model. The RANS models are not capable of reproducing the vertical gradient of temperatures present at the center of the physical model. This is better described using the DES turbulence model. The temperature above the cell near the building ceiling is also much closer in the DES model results (30.8 °C against 30.4–32 °C in the experiment), while the RANS model resulted in 27.3 °C at the same location.

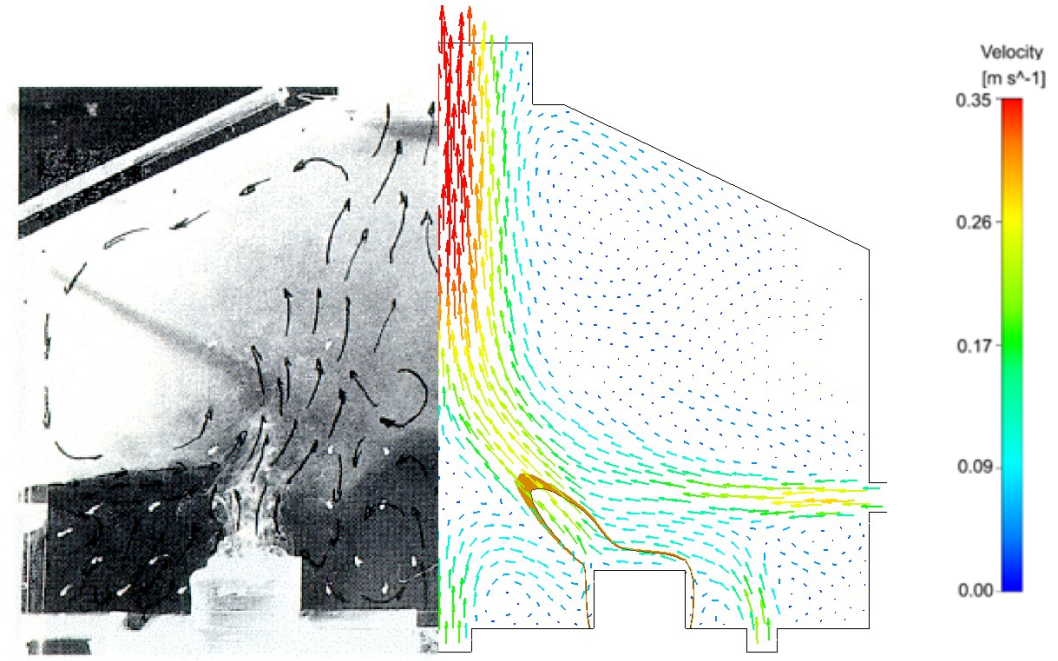

Figure 4. Qualitative comparison between experimental and Case A (RANS model) results. Vectors: time averaged air velocities. Plume: instantaneous isothermal surface at 36 °C.

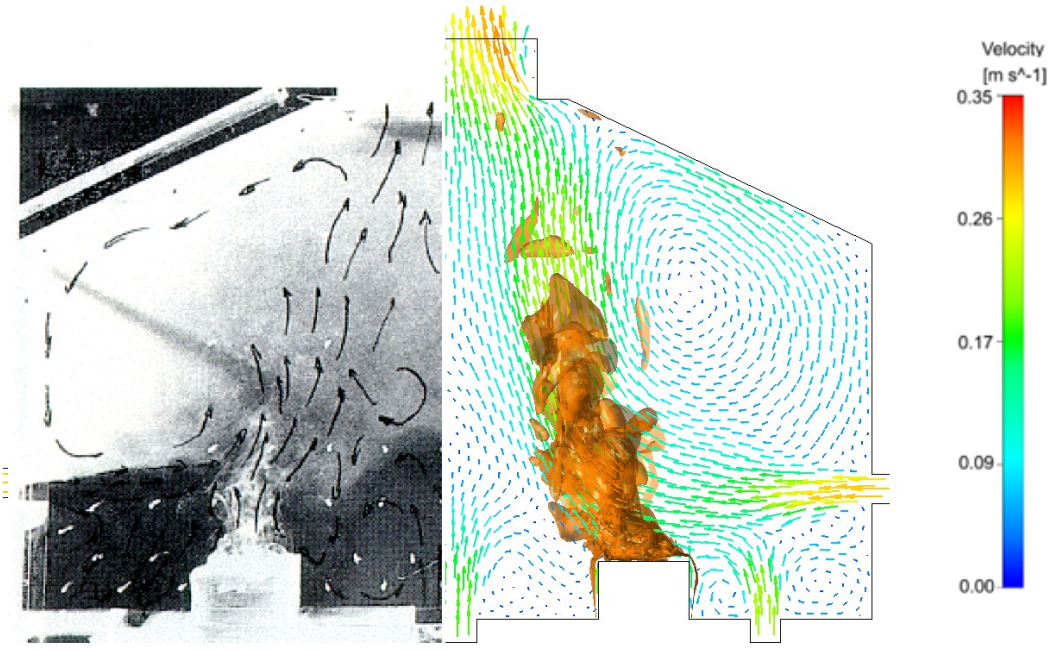

Figure 5. Qualitative comparison between experimental and Case D (DES model) results. Vectors: time averaged air velocities. Plume: instantaneous isothermal surface at 36 °C.

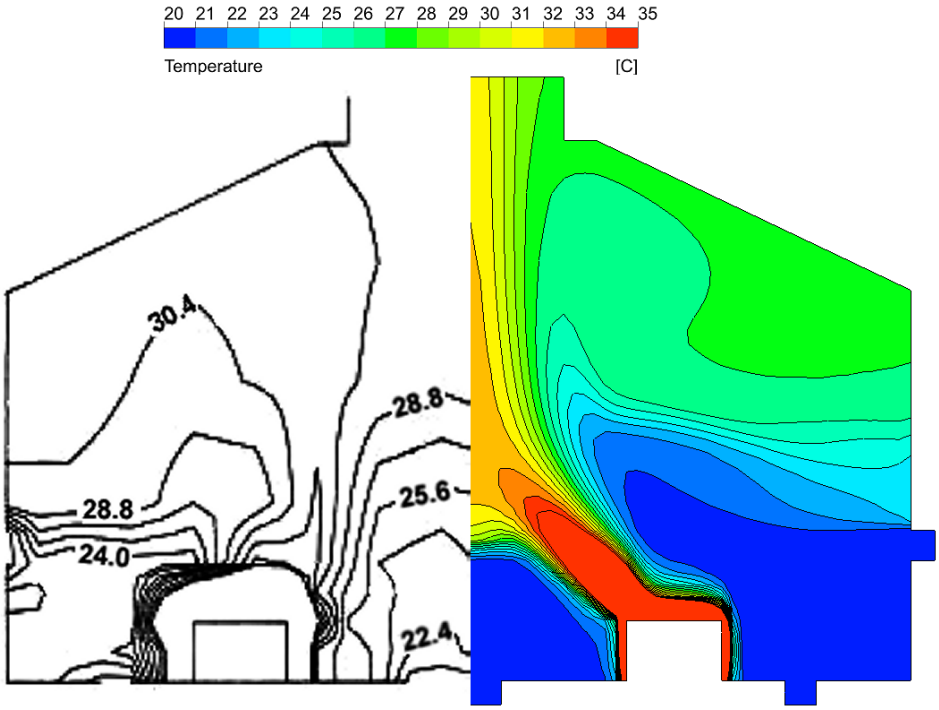

Figure 6. Results comparison. Left: measured temperature field. Right: air temperature field calculated using the RANS turbulence model (Case A).

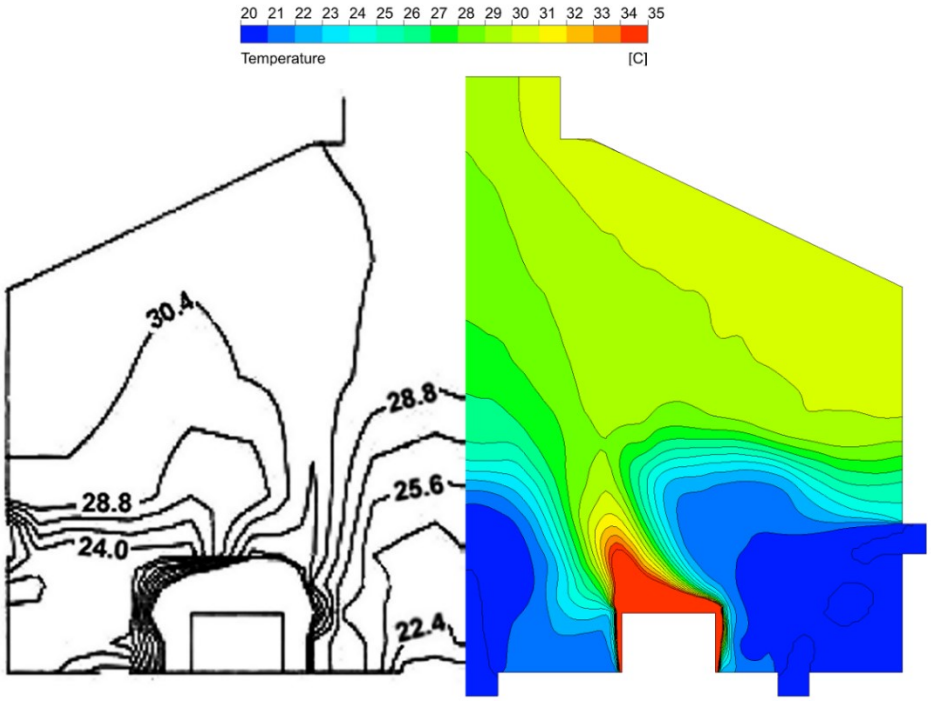

Figure 7. Results comparison. Left: measured temperature field. Right: time averaged air temperature field calculated using the DES turbulence model (Case D).

The approximate calculation times for each model are: Case A: 51 second, Case B: 35.7 hours, Case C: 97.1 hours and Case D: 36.2 hours. The simulations were run in personal computer AMD Ryzen Threadripper 1950X 16-Core Processor 3.40 GHz with 96 GB RAM memory.

4. Application of the Modelling Approach in an Industrial Potroom

The numerical modelling approaches developed and described in this work are applied in an industrial potroom case. Companhia Brasileira de Alumínio (CBA) has several Söderberg end-to-end reduction lines, where each potroom contains two potrows (the returning row is contained in the same potroom). This is a very similar disposition to the experimental physical model setup because the physical model was representing the old Kitimat smelter also using Söderberg cells.

The calculation domain corresponds to a slice of a potroom (*i.e.*, a typical unit of repetition in the center of a group of cells, away from passageways and potroom extremities), where one cell of each row is represented. In the modelling of the industrial potroom, the cell emissions are also simulated as numerical tracers by using the "variable mixture material" model available in the CFX code, where the user can add substances (species) that are transported by the flow velocities.

The boundary conditions (Figure 8) applied to the calculations are:

- Simulation is transient: 600 s are simulated using timesteps of 0.25 s.
- At the openings (bottom, windows, and top), averaged zero pressure condition is applied. The external temperature is set to 30 °C.
- Symmetry is applied at the potroom slice planes.
- At building walls, no slip (zero velocity) is applied for the fluid and the adiabatic condition is applied for the energy equation.
- At the cell walls, zero velocity for the fluid is applied. The total heat generation is 550 kW per cell, averaged over all cell surfaces. This value was estimated from previous heat balance modelling [9].
- Different external winds regimes are considered during the transient simulation: between 0 s and 200 s, no wind; between 200 s and 400 s, moderated wind; and finally, between 400 s and 600 s, strong wind is applied, according to Figure 9. The lateral wind is applied as a variable dynamic pressure at the opening surfaces. The wind has lower pressure near the ground due to boundary layer and the presence of obstacles in the smelter area. In order to represent this in the model, it has been postulated a distribution of wind pressure according to the opening height. At the bottom opening, 50 % of pressure is applied, at lateral window, 66 % is applied and at the roof opening 100 % of the dynamic pressure is applied. Zero pressure condition is maintained at the outlets.
- Hydrogen fluoride (HF) emission simulation: at the top of the bath channels, generation of 22 kg/day of hydrogen fluoride per cell is applied.

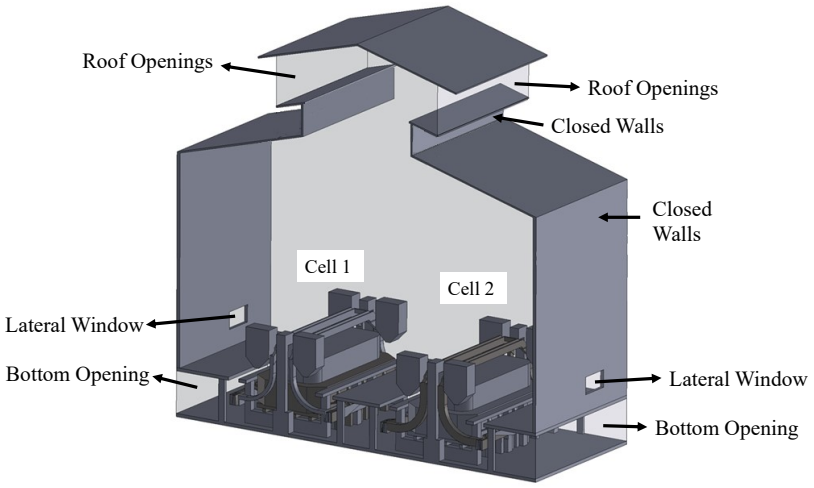

Figure 8. Sliced potroom model domain with boundary conditions at indicated regions.

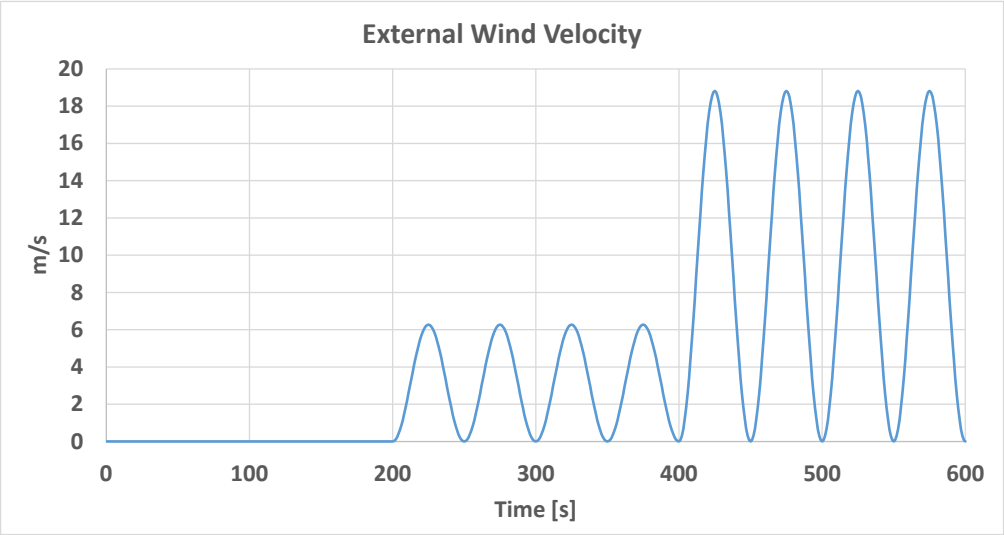

Figure 9. Wind magnitude regime applied in the potroom ventilation simulations.

For comparison, the two-equations turbulence model URANS SST k-omega and DES are used for the simulations: both models are transient and employed the same mesh. RANS models do not converge to a steady state solution when calculating the geometrically complex industrial potroom. In Figure 10, the instantaneous temperature plume is presented for both simulations with the abovementioned turbulence treatments. The air flow pattern is shown in black vectors for a plane cutting the building window, while the brown region corresponds to a 38 °C temperature isosurface. No external wind is considered here because the simulation timeframe is within the 0 to 200 s range. In Figure 11, the same type of comparison is presented but during the moderate wind phase of the simulation (200–400 s).

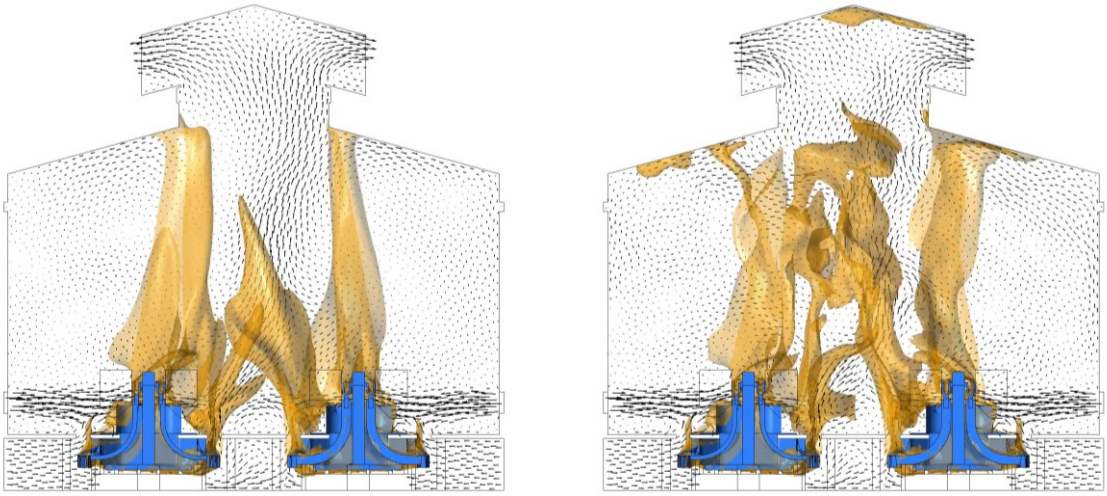

Figure 10. Temperature plume (isothermal surface at 38 °C) and flow pattern (black vectors, scale not shown). No wind. Left: SST k-omega turbulence model. Right: DES turbulence model.

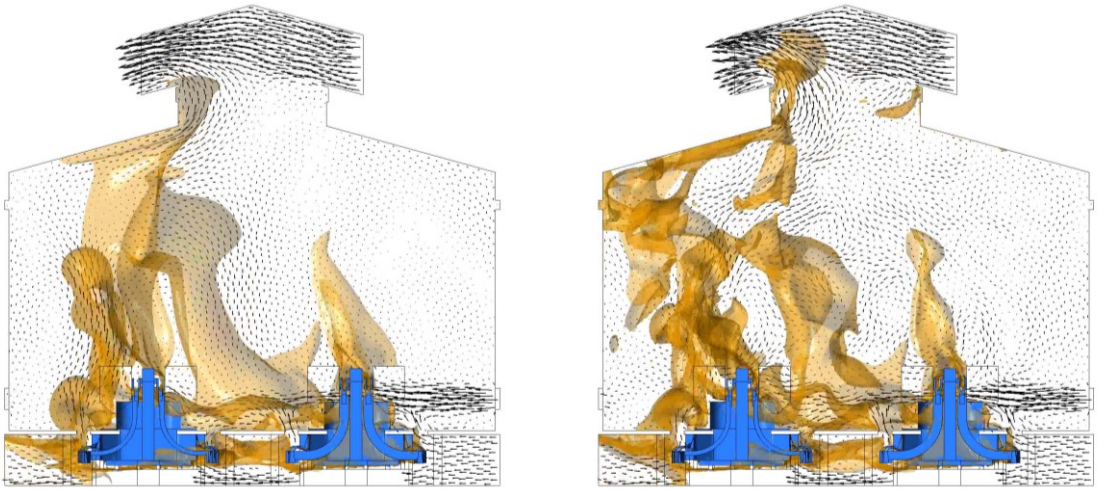

Figure 11. Temperature plume (isothermal surface at 38 °C) and flow pattern (black vectors, scale not shown). Moderated wind. Left: SST k-omega turbulence model. Right: DES turbulence model.

It can be observed that the SST k-omega result represents the natural convection flow in less detail than the DES result; using DES, the model is able to capture the main vortexes detachment, contrary to the transient two-equations turbulence models. This can be important, as it has been shown in the physical laboratory model, depending on the flow feature to be studied.

Similar to the temperature plume, contaminant plumes can also be simulated by using the tracer transport capability present in the CFX code. In Figure 12, for example, the instantaneous concentration of HF is shown in the green plume (iso-surface of 1.6 ppm) along with the velocity vectors in a center plane. Again, the DES turbulence model enables a much more detailed representation of both the velocity field and the HF concentration iso-surface compared with the SST k-omega turbulence model.

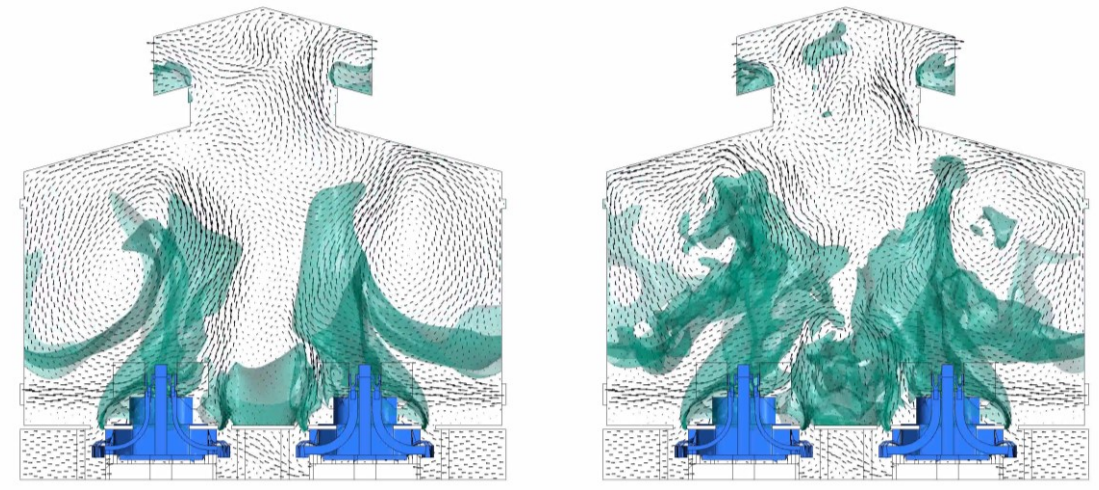

Figure 12. HF concentration iso-surface (1.6 ppm) inside the potroom after 45 s of simulation combined the flow pattern (black vectors, scale not shown). No wind. Left: SST k-omega turbulence model. Right: DES turbulence model.

The approximate calculation times for each model are: 87 h for the URANS model and 99 h for the DES model using the same computer described in the previous section, both using equal mesh and timestep size of 0.25 s. In the graphs in Figures 13 and 14, the HF mass flow passing through

each opening is monitored for both simulations of different turbulence treatments (SST k-omega and DES). The mass flow is obtained by integrating the concentration carried by the air velocity over the opening surface areas. The overall results appear to be very similar for both the studied cases. In the DES simulation, higher oscillation frequencies are present, which can be expected due to the nature of this numerical model, which captures the flow detachment from the plumes.

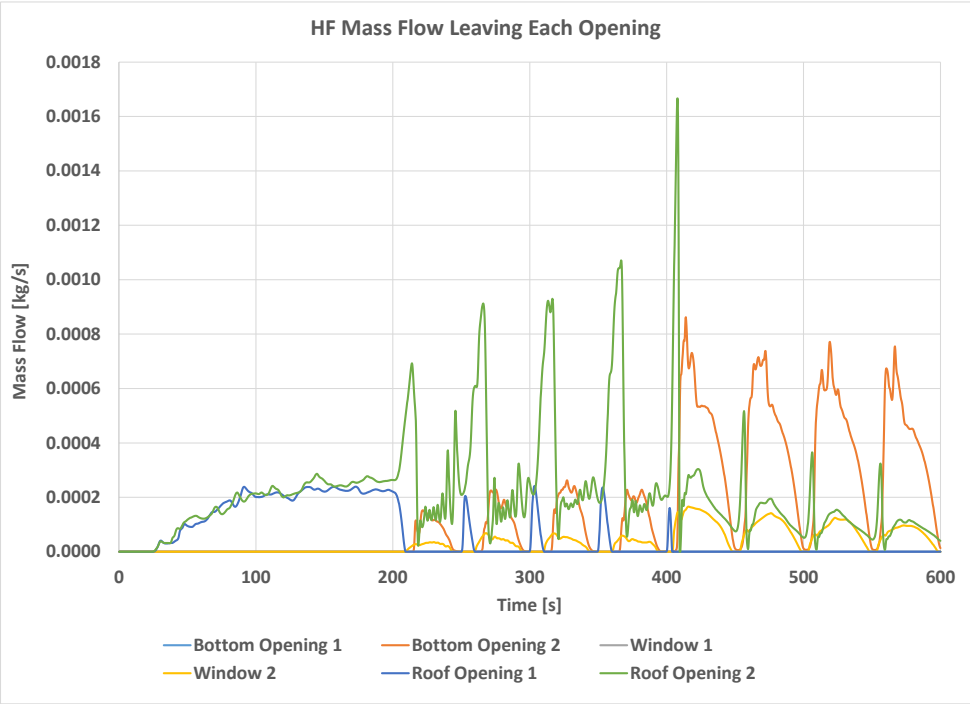

Figure 13. HF mass flow passing through each building opening over time. SST k-omega turbulence model.

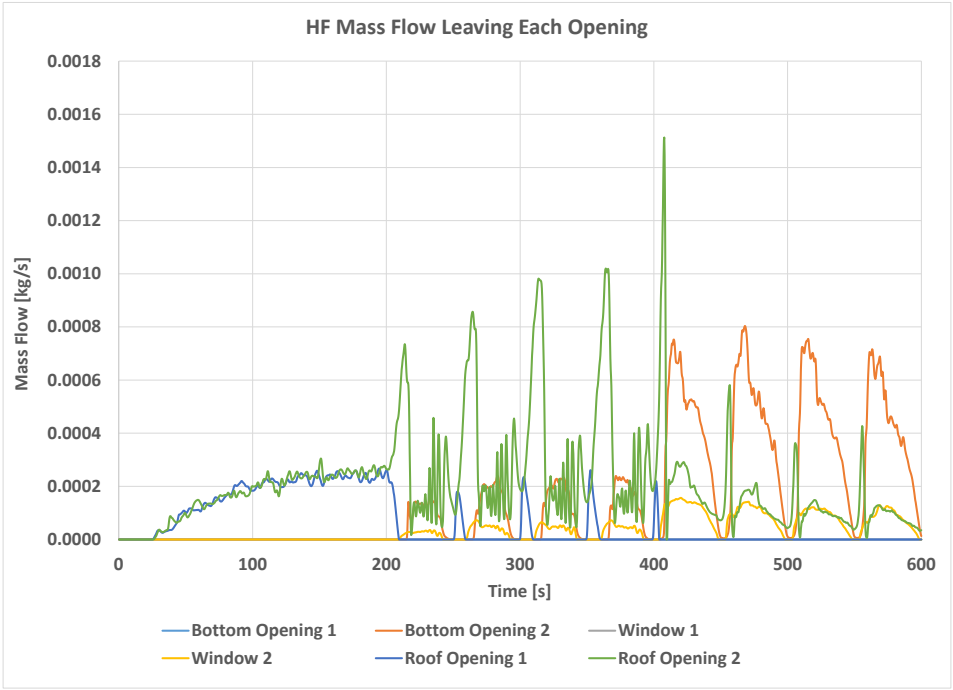

Figure 14. HF mass flow passing through each building opening over time. DES turbulence model.

In the graphs, it can be observed that during the no wind period (0–200 s), HF is leaving the building only through the roof openings, while during wind periods (200–600 s), HF can leave through the bottom opening and lateral window, opposite to the incident wind building side. This fact is summarised in Figure 15. The total mass of HF leaving the building through each opening was integrated over time during the simulation for both cases. The difference in the total HF masses is relatively small (less than 3 %), however this can indicate an important difference in flow behaviour. In the DES case, it appears that the HF has more difficulty reaching the roof opening, because of the higher complexity of the simulated air flow.

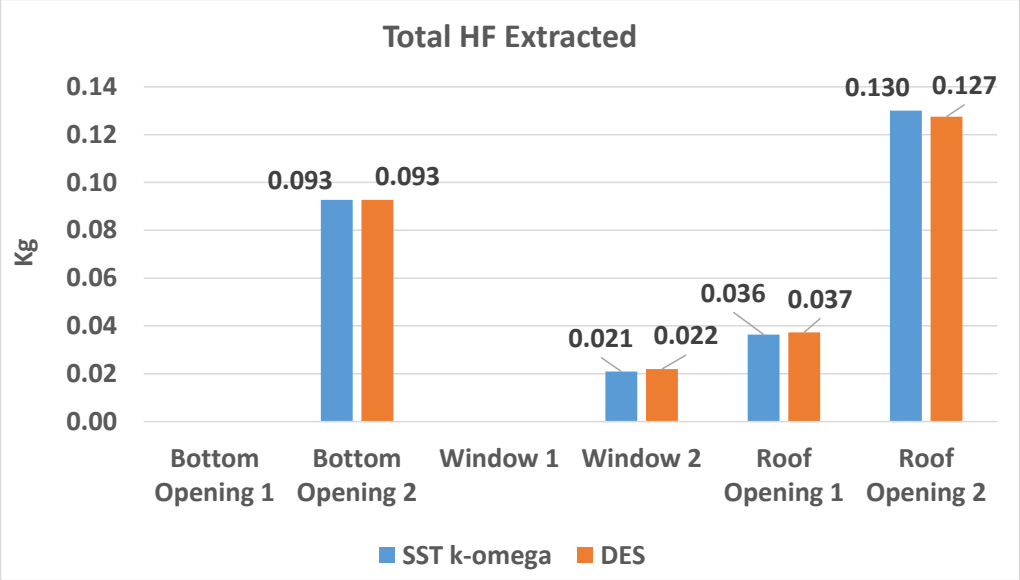

Figure 15. Total HF mass extracted at each building opening during the entire simulation period (0–600 s).

In the industrial case, the instantaneous DES velocity, temperature and concentration fields results are different and more complex when compared with the same URANS results, while the integrations overtime are more similar between both the models. This conclusion could be different in other geometries and boundary conditions. It is recommended to apply DES modelling as standard for future works as the computational effort is only moderately higher.

5. Conclusions

The natural convection flow produced in an industrial potroom is usually complex and highly turbulent. Simulation of this phenomenon is a challenging task. In particular, the choice of the turbulence modelling strategy defines the accuracy of the results and the level of flow features that can be described in time and space.

The comparison of the present modelling study with the past experimental work has shown that:

- The simple RANS models (k-epsilon, k-omega, SST k-omega, RSM) are inadequate to reproduce the main time-averaged features of the air flow.
- Only when using the LES or the hybrid model DES an accurate description of both the plume position and the vertical temperature gradients can be obtained.
- The large eddy detachment provided by LES or DES is an important feature of the flow and must be directly simulated to correctly position the plume.

The DES model was used to simulate natural convection in an industrial potroom. When compared with the URANS SST k-omega model, the DES model presents a more detailed description of the flow. However, the integrated contaminant massflow resulted to be very close in both the models. There is less discrepancy in this case because the pot superstructure is breaking the cross flow coming from the side windows. A steady state solution for the geometrically complex model of the industrial potroom does not exist. This is because the large eddies are intermittently formed and dissipated by the natural convection. Only a transient numerical simulation predicts these flow structures.

In industrial applications, analysts have to carefully choose the turbulence models according to the simulation objectives, the desired degree of detail in the flow description, and the computational effort required for the task. In future works, the authors intend to demonstrate the behaviour and applicability of the turbulence models in side-by-side potlines, where a single potrow is commonly placed in the building, in an asymmetric position with respect to the vertical building's center plane. This potroom arrangement may present a different flow pattern from the results present in this work.

6. References

1. Marc Dupuis, Edgar Dernedde and J. C. Methot, La modélisation de la turbulence dans une enceinte avec ouvertures et sources chaudes localisées, *Can. J. Chem. Eng.,* 67, (1989), 713–721.
2. Marc Dupuis, J. C. Méthot and Edgar Dernedde, Simulation mathématique de la circulation de l'air dans une enceinte avec ouvertures et sources chaudes localisées, *Can. J. Chem. Eng*., 63, (1985), 155–161.
3. Marc Dupuis, Edgar Dernedde and Diane S. Clarke, Turbulence modeling of air circulation in an enclosure with multiple openings and local heat sources, *CIM Light Metals*, 1993, 229–236.
4. Marc Dupuis, 3D modeling of the ventilation pattern in an aluminum smelter 'potroom' building using CFX-4", *CFD 2001 Conference*, Canada, Waterloo, Ontario, May 27–29, 2001.
5. Jon Berkoe et al., CFD modeling of the Fjardaal smelter potroom ventilation, *Light Metals* 2005, 373–378.
6. Nathalie Menet et al., Latest developments in potroom building ventilation CFD modelling, *Light Metals* 2013, 811–816.
7. André van Maarschalkerwaard, The use of CFD simulations to optimize ventilation of potrooms", *Light Metals* 2010, 423–426.
8. Anastasiya Vershenya et al., Modern design of potroom ventilation, *Light Metals* 2011, 531–535.
9. Dagoberto S. Severo et al., Thermal behavior of cathode bottom lining at CBA, *Proceedings of the 36th International ICSOBA Conference,* Belem, Brazil, 29 October - 1 November, 2018, *Travaux* 47*,* 693-706.